Direct Intensity Detection of Complex Communication Data Signals Using a Real-time Photonics Spectrogram

Connor M.L. Rowe, Benjamin Crockett, José Azaña
Énergie, Matériaux et Télécommunications – Institut National de la Recherche Scientifique, 1650 Blvd Lionel-Boulet, J3H5Z2 Varennes, Québec, Canada
connor.rowe@inrs.ca

Abstract: We use a time-lens spectrogram for real-time recovery of complex modulation data signals using a single photodiode, no local oscillator, and simple decision method. Our proof-of-concept experiment decodes QAM4 and QAM8 under the FEC limit. © 2022 The Authors

1. Introduction

The growing demand in communication capacity of data centers and networks requires practical implementation of complex modulation to increase the information density per symbol. Controlling not just the intensity, but also the phase of a carrier wave, provides a second dimension for data encoding, increasing the spectral efficiency. The current standard for decoding complex-modulated data signals is coherent detection [1], where a phase stable local oscillator is used to create an interferometric system to recover the in phase and quadrature (I and Q) components of the signal. There are many permutations of the basic conceptual design, but most involve multiple balanced photodetectors, a stable phase-coherent local oscillator, and energy-consuming DSP engines [2], yielding costly and complex receivers [3]. Furthermore, increasing modulation order places increasing demands on the local oscillator linewidth for many coherent detection schemes, and thus it would be ideal to remove the local oscillator entirely [3].

Spectrograms (involving intensity-only information) are known to enable the retrieval of the phase information of a signal. This strategy has been used previously for complex-field characterization of ultrafast optical waveforms (such as in FROG [4]) with enormous success. However, optical implementations of spectrogram are limited to finite duration waveforms (such as short pulses), prohibiting their use for decoding telecommunication data signals [5]. Recently, we developed a novel technique enabling time-frequency analysis of broadband waveforms without any restriction on maximum signal duration called the time lens spectrogram (TLS) [6]. Here we demonstrate this capability by recovering the phase information of complex-modulation telecom data signals from the photo-detected spectrogram of the signal of interest, in a colorless fashion (i.e., regardless of carrier frequency). The key principle relies on measuring the optical spectrum of each transition from one symbol to the next; in other words, we implement a differential detection scheme based on the spectral content of each transition. Since each symbol transition has a unique spectrum (that is, power spectrum), it is possible to decode the next symbol by comparing the current spectrum with the set of possible unique spectra. As an a experimental proof-of-concept, we demonstrate the decoding of 1 Gbaud/s QAM4 and QAM8 signals with pre-FEC BER of $<5.96\times 10^{-8}$ and 2.00×10^{-4} respectively, within acceptable limits for FEC [7].

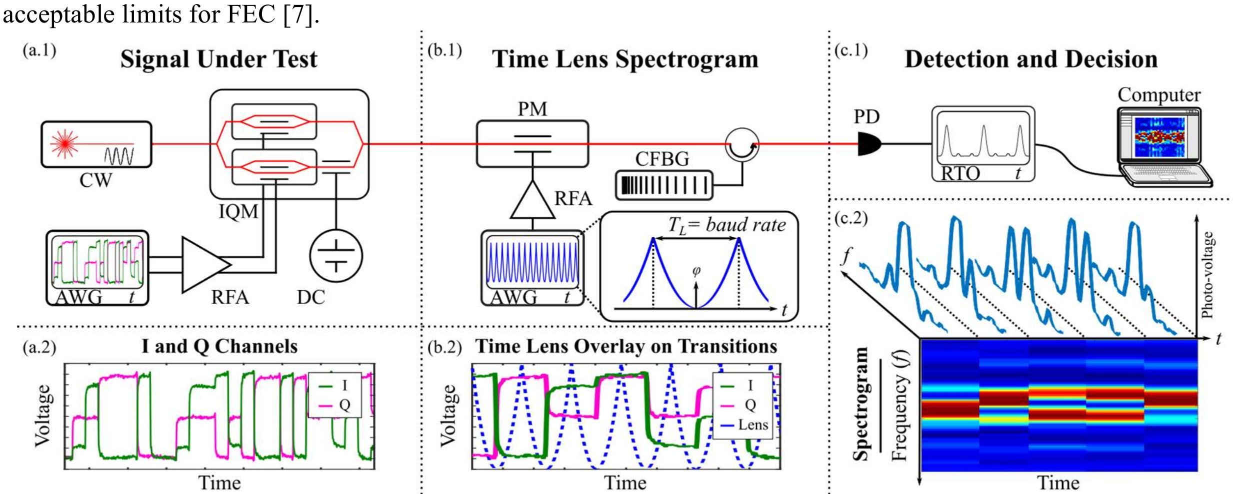

Figure 1. **a.1** Complex data signal generation. **a.2** The electrical I and Q channels as voltage over time. **b.1** The time lens spectrogram optical components. **b.2** The alignment of the time lens with the complex data signal so that each lens images the transition from one symbol to the next. **c.1** Detection and hard decision method by cross correlation with a known set of transitions. **c.2** The time lens spectrogram results in the spectra of each transition mapped to the time domain, which are positioned as shown to produce a spectrogram. Acronyms defined in main text.

2. Operation Principle

The TLS is realized by first modulating the temporal phase over consecutive periods T_L according to a quadratic function $\varphi(t) = i(C_L/2)t^2$, where C_L is the strength of the modulation, shown in Fig. 1 (b.1). This is implemented using an electro-optic phase modulator (PM) driven by an arbitrary waveform generator (AWG) and a radio-frequency amplifier (RFA). The second portion of the TLS consists of a chirped-fiber Bragg grating (CFBG) providing a spectral phase filter following $\phi(\omega) = i(\ddot{\phi}/2)\omega^2$, where $\ddot{\phi}$ is the second-order group velocity dispersion parameter, corresponding to the slope of the group delay vs radial frequency. Under the imaging condition $\ddot{\phi}C_L = 1$, the output spectrum of a signal with a maximum analysis bandwidth $\nu_L = C_L T_L/(2\pi)$ (i.e., limited to the maximum phase excursion of the time lens modulation) will be mapped to a maximum time duration T_L according to the well-known frequency to time mapping law $2\pi\nu = t/\ddot{\phi}$, where ν and t are taken relative to the center of the lens [5]. The use of a time-lens array consisting of adjacent quadratic phase modulations, as shown in Fig. 1 (b.1), ensures realization of a gapless spectrogram, in which no information of the incoming analyzed signal is lost. The resulting signal (time-mapped spectrogram) is detected using a single photodiode (PD) (i.e., intensity only measurement) connected to a real-time oscilloscope (RTO), depicted in Fig. 1(c1). To create the final spectrogram image, each spectrum can be plotted vertically as shown in Fig. 1 (c.2). Note that the TLS retrieves the double-sided spectrum, as shown in the first part of Fig. 1 (c.2), which provides sufficient information about the phase content of the signal to decode the data stream. In the specific scheme proposed here for phase retrieval of a telecommunication data signal, the temporal phase modulation signal is aligned such as to obtain the spectrum of each transition, see Fig. 1 (b.2). A decision algorithm based a simple cross-correlation is then implemented offline on a computer in order to compare each time-mapped transition to a known set of unique transitions that were recorded beforehand.

3. Results

To generate the data signal to be recovered, a Keysight AWG with a 92 GS/s rate was used to drive a 10 GHz IQ which modulated a continuous wave carrier (CW) laser at 1550 nm. This signal was then sent to the TLS which consisted of a 40-GHz electro-optic phase modulator, and two concatenated chirped fiber Bragg gratings providing a total dispersion of 15,713 ps^2. The time-mapped spectra were detected using a 50 GHz photodiode and recorded using a 28 GHz real-time oscilloscope. The cross correlation was implemented in the post-processing on a computer but could readily be implemented in real time. To calculate the final pre-FEC BER, we divide by the modulation order (i.e., number of bits per symbol) as is standard for a gray coded signal. It is well-know that forward error correcting codes (FEC) allow many orders of magnitude improvements in bit error rate [3], and thus, it is standard to judge a method based on pre-FEC bit error rates (BER).

We demonstrate first the recovery of a QAM4 pseudo-random bit sequence (PRBS) signal operating at 1 Gbaud/s with a length $2^{23} - 1$. A sample of the electrical AWG signal is used to plot the constellation diagram of this PRBS in Fig. 2. (a.1), indicating a high SNR. The spectrogram of this waveform (i.e., the output of the TLS) is shown in Fig. 2. (a.2), where the vertical slices correspond to the spectra of the transition from one bit to the next. The bit sequence shown in Fig. 2. (a.2) is the calibration sequence, which gives the library of all possible transitions for this modulation format. The averaged unique transitions from the calibration sequence are shown to the right of the spectrogram image in Fig. 2 (a.2) along with their corresponding phase changes. Notice the transition corresponding to a π-phase shift gives the broadest spectral distribution, which is also symmetric. On the other hand, smaller phase transitions give a spectrum that is peaked at a lower frequency, in the positive or negative frequency direction, depending on whether the transition corresponds to an upwards or downwards chirp, respectively. In Fig. 2 (a.3), we plot the similarity between transitions of two separate calibration sequences, to evaluate the fidelity of the method and identify possible transitions which may cause errors. Two calibration sequences recorded at different times are used for the similarity map to account for expected variations of the signal generation in time. For QAM4 we can see that there is very little ambiguity between transitions. This corroborates the efficacy of the TLS for recovery in this proof-of-concept demonstration, as no errors were detected in the entire length of the PRBS analyzed. The estimated pre-FEC BER for the QAM4 signal is therefore $< 5.96 \times 10^{-8}$.

For a signal with smaller phase variations and thus a denser set of spectral patterns for unique transitions, which also includes intensity variations, we target the recovery of a QAM8 data signal. The constellation diagram of a PRBS of length $2^{20} - 1$ is shown in Fig. 2. (b.1). Part of the spectrogram of the calibration sequence is shown in Fig. 2. (b.2), along with the averaged unique transitions, of which there are 8 total. The vertical cutoff seen in the unique transition spectra are due to the intentional saturation of the real-time oscilloscope to obtain more dynamic range in the vertical region containing the differentiable features. The similarity map of the transitions is shown in Fig. 2. (b.3). The similarity map accounts for the increased error rate as the transitions are more difficult to discern from one another

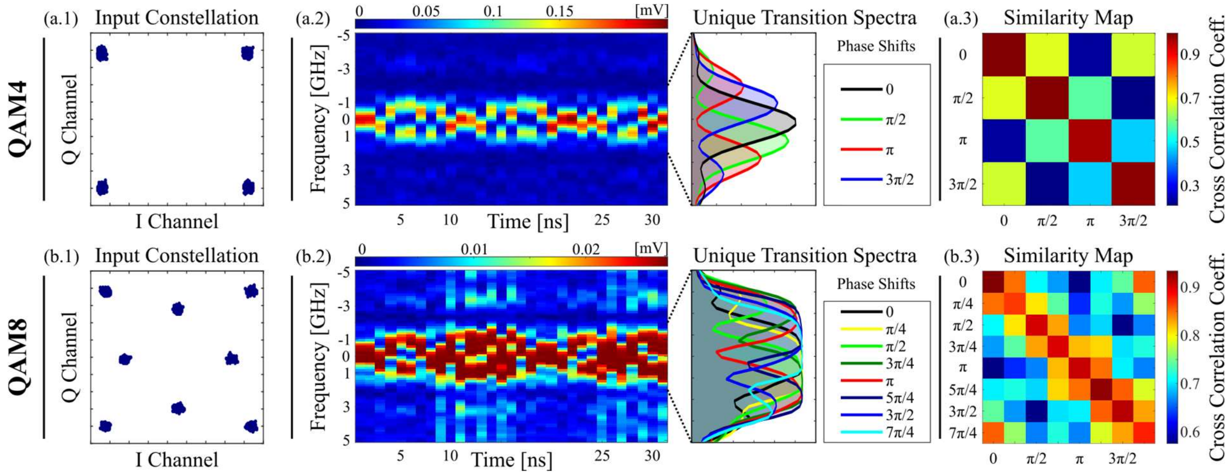

Figure 2. **a.** QAM4 results. **a.1** The input constellation diagram directly from the electrical outputs of the AWG generating the signal under test. **a.2** The spectrogram for the calibration bits is shown, as well as the averaged transition from all transitions resulting in the same phase change. **a.3** The similarity map generated by comparing each transition of one calibration sequence to each of a different sequence via cross correlation is shown. **b.** QAM8 results. **b.1** Constellation diagram of the input signal, showing multiple intensity levels. **b.2** Spectrogram for a subset of the calibration sequence (31 transitions out of 127) and averaged unique transitions. **b.3** Similarity map.

in the case of higher modulation order of QAM8. Still, the pre-FEC BER for the QAM8 signal was 2.00×10^{-4}, within the standard pre-FEC limit for QAM detection, showing that the technique can enable the detection of more sophisticated modulation schemes.

4. Discussions and Conclusion

Using the TLS, we have demonstrated a proof-of-concept experiment for the recovery of the phase information of complex data signals from intensity-only measurements based on a time-frequency analysis approach. We have successfully applied this method to QAM signal recovery, requiring no local oscillator, a single photodetector, and a simple hard decision method, regardless of carrier frequency. This system greatly simplifies the hardware requirements without relying on computationally intensive DSP. We anticipate this scheme is viable for successful recovery in the case of noisy, low intensity, and dispersion corrupted signals. We also anticipate recovery of higher order QAM16 data signal formats using the specific strategy reported here, but we note that there are pertinent challenges in this direction. Specifically, as the TLS analysis rate is set to be the baud rate of the data signal, the bandwidth of a transition will be within a fraction of the total analysis bandwidth of the TLS. Considering the minimum frequency resolution, there is a corresponding limited number of analysis points relevant to the transition spectra. For higher order modulations, the number of unique spectral signatures increases without any increase in the bandwidth that they cover, making them increasingly difficult to recover. However, we predict that a more sophisticated lens system, as well as other methods specifically tailored to recovering complex communications data signals from a spectrogram, could be considered. To our knowledge, we have reported here the first demonstration of the use of real-time joint time-frequency signal analysis for the recovery of complex-modulation optical data signals using self-referenced intensity-only measurements, thus opening the path for further developments of this promising approach.

5. References

[1] K. Kikuchi, 'Fundamentals of Coherent Optical Fiber Communications', *J. Light. Technol.*, vol. 34, no. 1, pp. 157–179, Jan. 2016.

[2] B. Puttnam *et al.*, 'Self-Homodyne Detection in Optical Communication Systems', *Photonics*, vol. 1, no. 2, pp. 110–130, May 2014.

[3] K. Kikuchi, 'Coherent Optical Communications: Historical Perspectives and Future Directions', in *High Spectral Density Optical Communication Technologies*, M. Nakazawa, K. Kikuchi, and T. Miyazaki, Eds. Berlin, Heidelberg: Springer Berlin Heidelberg, 2010, pp. 11–49.

[4] R. Trebino, *Frequency-Resolved Optical Gating: The Measurement of Ultrashort Laser Pulses*. Boston, MA: Springer US, 2000.

[5] R. Salem, M. A. Foster, and A. L. Gaeta, 'Application of space–time duality to ultrahigh-speed optical signal processing', *Adv. Opt. Photonics*, vol. 5, no. 3, p. 274, Sep. 2013.

[6] C. M. L. Rowe, B. Crockett, and J. Azaña, 'Photonic-Enabled Real-time Spectrogram Analysis of sub-Nanosecond Microwave Events over a 40-GHz Instantaneous Bandwidth', in *2022 IEEE/MTT-S International Microwave Symposium - IMS 2022*, 2022, pp. 833–836.

[7] T. Mizuochi, 'Recent progress in forward error correction and its interplay with transmission impairments', *IEEE J. Sel. Top. Quantum Electron.*, vol. 12, no. 4, pp. 544–554, Jul. 2006.